Available online at www.sciencedirect.com
SCIENCE DIRECT®
Journal of Nuclear Materials 342 (2005) 35–41
journal of nuclear materials
www.elsevier.com/locate/jnucmat

Dislocation structures in 16MND5 pressure vessel steel strained in uniaxial tension

K. Obrtlik [a], C.F. Robertson [b,*], B. Marini [b]

[a] *Institute of Physics of Materials, Academy of Sciences of the Czech Republic, Zizkova 22, 616 62 Brno, Czech Republic*
[b] *Commissariat á l'Energie Atomique/Saclay, SRMA bât. 455, 91191 Gif-sur-Yvette, France*

Received 27 September 2004; accepted 11 March 2005

Abstract

Cylindrical specimens of bainitic pressure vessel steel 16MND5 were strained in uniaxial tension at liquid nitrogen temperature. Dislocation structures and surface relief were studied at 2.5% and 8% of plastic deformation and their evolution with increasing plastic strain is documented. The knowledge of dislocation arrangements is the starting point to model the local stress states that can result in cleavage initiation.

1. Introduction

Bainitic steel 16MND5 is used to manufacture the pressure vessels of pressurized water nuclear reactors. This material undergoes a ductile to brittle transition (DBT) in the fracture mode with decreasing temperature and/or increasing strain rate. In addition, neutron irradiation embrittlement induces an increase of the DBT temperature. Therefore, the prevention of brittle fracture of the steel is a fundamental issue in nuclear plant life management. Generally, the brittle fracture in pressure vessel steels has a cleavage character. Most cleavage mechanisms mentioned in the literature involve local crystal plasticity associated with the generation, motion and interaction of dislocations [1].

In α-iron, it is known since many years that the behaviour of dislocations is temperature dependent. Dislocation structures developed in uniaxial straining at low temperature were studied both in single crystals and polycrystals of pure iron [2,3]. At low temperature, the dislocation distribution is rather uniform. The individual dislocations, mainly of screw character, are relatively straight and lie on crystallographic planes. The dislocation density is slightly larger in the fine grained than in the coarse grained material. With increasing strain, dislocations soon gather into clusters or walls. Data on dislocation structure in bainitic steel at low temperature are missing. This material is made of packets of laths or blocks, therefore, a significant effect of the internal interfaces on the dislocations arrangements is expected.

The aim of the present study is to investigate the arrangement of dislocations in bainitic 16MND5 steel strained in uniaxial tension at low temperature. The development of dislocation structures and surface relief with increasing strain is reported and discussed. The present work is part of a more complex project, dealing

* Corresponding author. Tel.: +33 1 69 08 22 70; fax: +33 1 69 08 71 67.
E-mail address: christian.robertson@cea.fr (C.F. Robertson).

0022-3115/$ - see front matter © 2005 Elsevier B.V. All rights reserved.
doi:10.1016/j.jnucmat.2005.03.010

with the behaviour of the steel in the DBT temperature regime. The knowledge of dislocation arrangements is needed to model the local stress states that can be associated with cleavage initiation.

2. Experimental details

16MND5 steel (US denomination: A508CL3) was taken from a pressure vessel nozzle cut off. After forging, the heat treatment of the material was the following: twice austenization at 865/895 °C for 4 h 30 min and water quenched, then tempering at 630/645 °C for 7 h 30 min followed by stress relieving at 610 °C for 8 h.

The heat treatment resulted in a bainitic microstructure, made of packets of parallel ferritic laths. The typical individual lath is 10×10 μm^2 with a lath thickness of 1–2 μm. In this paper, the direction parallel to the lath thickness is labelled as the *c* axis. Carbides are present in the form of both needles and globular particles, having the mean diameter of 0.1 μm. These particles partially cover the lath boundary planes (about 80%) where they can act as obstacles to slip. The individual lath disorientation inside a given packet of laths is nowhere larger than 5°. Original austenitic grain size was evaluated to be 50 μm. Inclusions up to 10 μm in size are present. The initial dislocation densities in the material are low: dislocations were present mainly at the lath or packet boundaries.

The material composition is given in Table 1. The cylindrical specimens with threaded ends had gauge diameters of 4 mm. Fig. 1 shows the specimen dimensions. The specimen loading axis is parallel to the surface of the pressure vessel ring, in the transverse direction. The tensile tests were performed in an electro-hydraulic testing machine INSTRON at a rate of 5×10^{-5} s^{-1} up to the plastic strains of 2.5% and 8%. In this study, most of the tests have been carried out in liquid nitrogen (−196 °C). Some additional testing at 0 °C has been performed for comparison and discussion purposes. A complete characterization including tensile tests on axisymmetrically notched specimens and fracture toughness tests on CT specimens at low temperatures of the material under study were reported elsewhere [4].

Surface relief evolutions were examined in a mechanically polished specimen, using diamond paste down to 1 μm particle size. The tensile test of the specimen was stopped at the completion of plastic strains of 2.5%

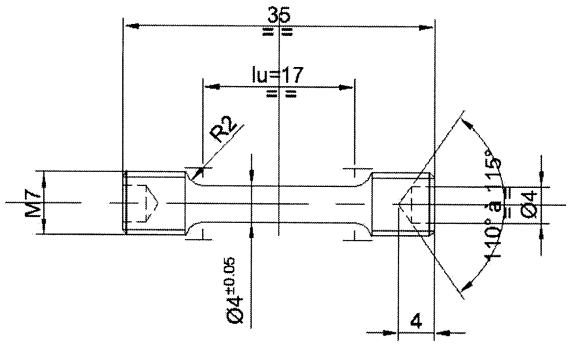

Fig. 1. Shape and size of the specimen (in mm).

and of 8% and the specimen was removed from the testing machine for observation in SEM 260 Stereoscan. Dislocation structures were observed in TEM Philips CM-20 operating at 200 kV, using a double tilt holder. Thin foils were prepared using the standard double jet technique from specimen slices cut at an angle of 45° to the specimen axis. Special care was taken to mark the specimen so that the orientation of each lath relative to the loading axis could be determined using diffraction patterns and Kikuchi lines. The usual notation in which the loading axis is within the basic stereographic triangle (0 0 1), (−1 1 1), (0 1 1) was adopted.

3. Results

3.1. Stress–strain curve

The experimental load-elongation curve was converted into a stress–strain curve, under the assumption of uniform elongation of the gauge length. Fig. 2 shows the stress–strain curve of the steel obtained at liquid nitrogen temperature testing. High yield point, larger yield drop and elongation zone are characteristic for low temperature tension test of the steel, in agreement with the behaviour of other bcc metals [5].

3.2. Dislocation arrangements: 2.5% plastic strain

The steel was characterized by low dislocation density in individual laths, before the tensile tests. Dislocations were present mainly at the boundaries of laths and packets. An example of dislocation arrangement before tensile test is shown in Fig. 3. In addition to the disloca-

Table 1
Composition of 16MND5 steel (wt%)

C	S	P	Mn	Si	Ni	Cr	Mo	V	Cu	Co	Al
0.16	0.008	0.005	1.38	0.24	0.70	0.17	0.50	0.005	0.06	0.01	0.020

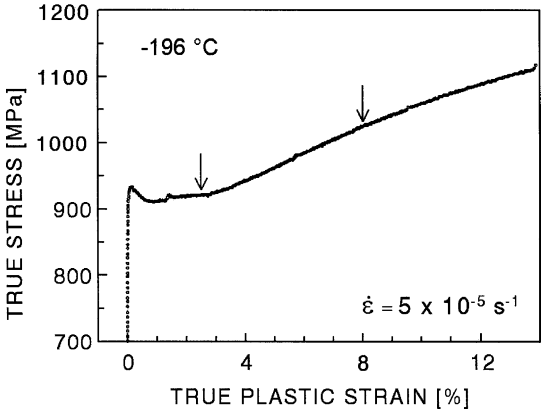

Fig. 2. Stress–strain curve of the steel.

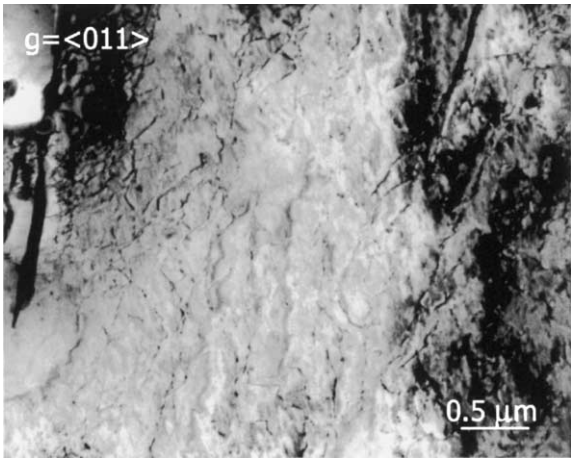

Fig. 3. Dislocation structure within a lath before tensile test. The lath *c* axis is perpendicular to the foil plane.

tions at the lath boundaries, few very fine rows of dislocations are present within the lath. These rows may later form nuclei of dislocation walls that are frequent in the deformed material. TEM investigation reveals that dislocation distribution in individual specimens at both values of plastic strain (2.5% and 8%) is characterized by strong heterogeneity. Namely, dislocation poor regions alternate with regions having high dislocation density, whereas the dislocation densities also vary from a bainitic lath to a lath. The strain heterogeneity depends on plastic strain. The fraction of grains with high dislocation density increases with increasing amount of deformation. Attention was concentrated mainly on the regions with high dislocation density.

Dislocation arrangement typical for liquid nitrogen temperature and plastic strain of 2.5% is shown in Fig. 4(a). The lath is oriented for single slip – with a [−1 5 7] tensile axis. The Schmidt factor of the primary

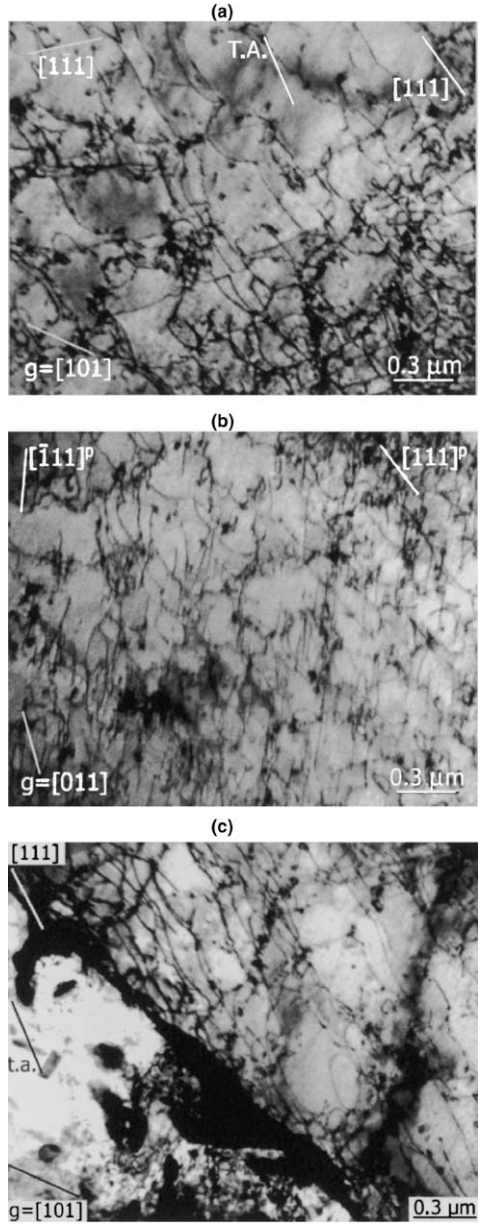

Fig. 4. Characteristic dislocation structure in a lath after 2.5% tensile test at −196 °C: (a) beam direction [−4 3 4], g = [1 0 1], lath *c* axis is perpendicular to the foil plane; (b) beam direction [−5 2 2], g = [0 1 1], t.a. is tensile axis and $[1\,1\,1]^p$ means the projection of the direction [1 1 1] into the image plane, the lath *c* axis is perpendicular to the foil plane; (c) interactions between screw dislocations and inter-lath carbides, beam direction [−1 0 1], g = [1 0 1], the lath *c* axis is parallel to the foil plane. Note the series of aligned debris loops in the upper part of the micrograph.

slip system [1 1 1] (−1 0 1) is 0.48, the ratio of the resolved shear stress of the second most stressed system is 0.89.

The foil plane $(-10,1,11)$ is close to the primary slip plane. Dislocations with Burgers vector of $a/2[1\,1\,1]$ and $a/2[1\,-1\,1]$ are visible in the diffraction condition of g = [1 0 1]. Projection of directions of both Burgers vectors into the image plane is shown in the left and right upper corners. The dislocation arrangements visible in Fig. 4(a) mainly consist in uniformly distributed screw dislocations, with Burgers vector of the primary slip system. The straight individual screw dislocation segments are about 500 nm long. Dislocations of the coplanar slip system with b = $a/2[1\,-1\,1]$ are sporadic, since their Burgers vector is almost perpendicular to the tensile axis. Therefore, the value of the Schmidt factor of slip systems with b = $a/2[1\,-1\,1]$ is very small.

Dislocations with Burgers vector of secondary slip systems are nevertheless present in their slip planes without being apparent in Fig. 4(a). Fig. 4(b) shows an example of dislocation arrangement obtained in the diffraction condition of g = [0 1 1], from the same place of the lath as in Fig. 4(a). Dislocations having the secondary slip system Burgers vector b = $a/2[-1\,1\,1]$ are visible, in addition to dislocations having the Burgers vectors of the primary slip system b = $a/2[1\,1\,1]$. The average spacing between dislocations with Burgers vector b = $a/2[-1\,1\,1]$ is 100 nm.

In Fig. 4(a), debris in the form of 10–100 nm dislocation loops are clearly visible in addition to the straight screw segments. In Fig. 4(c), series of aligned debris loops left behind by the moving screw dislocations are visible as well. This micrograph also shows that slip transmission from one lath to the next one is blocked at the lath-carbides interface, even though the two neighbouring laths have nearly the same crystalline orientation.

In Fig. 5, dislocation structures within laths from two specimens strained to 2.5% at −196 °C and 0 °C are compared side to side. This comparison clearly shows that the length of straight screw segments is significantly reduced when the test temperature is increased, likely due to increased kink pair nucleation.

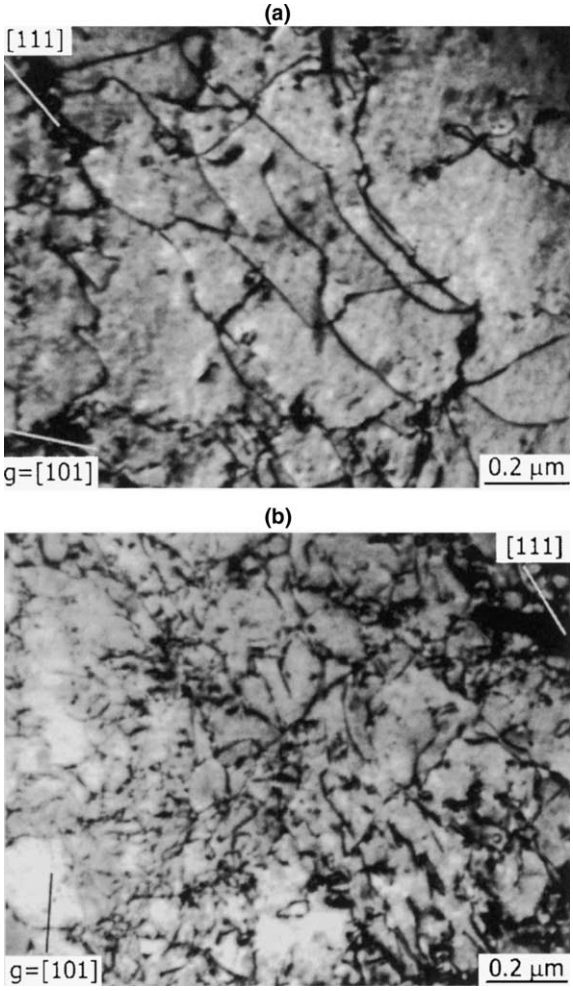

Fig. 5. Slip at 2.5% plastic strain at two different temperatures: (a) −196 °C, beam direction [−1 0 1], g = [1 0 1], the lath c axis is perpendicular to the foil plane; (b) 0 °C, beam direction [−1 0 1], g = [1 0 1], the lath c axis is perpendicular to the foil plane.

3.3. Dislocation arrangements at 8% plastic strain

Fig. 6(a) shows an example of dislocation arrangement associated with the test temperature of −196 °C and the plastic strain of 8%. Diffraction condition of g = [1 1 0] implies that dislocations with the Burgers vector $a/2[1\,1\,1]$ of the primary slip system and dislocations with the Burgers vector $a/2[-1\,-1\,1]$ of the secondary slip system are visible. Dislocations have the same character as at low strain (see Figs. 4 and 5(a)) but they are no longer distributed homogeneously within the lath and condensation into walls is clearly apparent (see Fig. 6(a)). These walls can also interact with the carbides present at the lath boundary, as shown in Fig. 6(b).

3.4. Surface observations

Several markers were made on the specimen surface to facilitate localization of small, specific zones. Fig. 7(a) shows the surface of the specimen strained to the plastic strain of 2.5%, at −196 °C. A few wavy slip markings are visible in the surface. The fraction of laths containing surface slip markings is very low, about 10%. Some of the micron size inclusions (carbides) aligned with the markings (not shown here) are cracked. Fig. 7(b) shows evolution of the surface relief in the same place after the plastic strain of 8% was achieved. The density of slip markings increases with increasing plastic strain, whereas some original markings become more pronounced, showing a certain degree of persistency. It

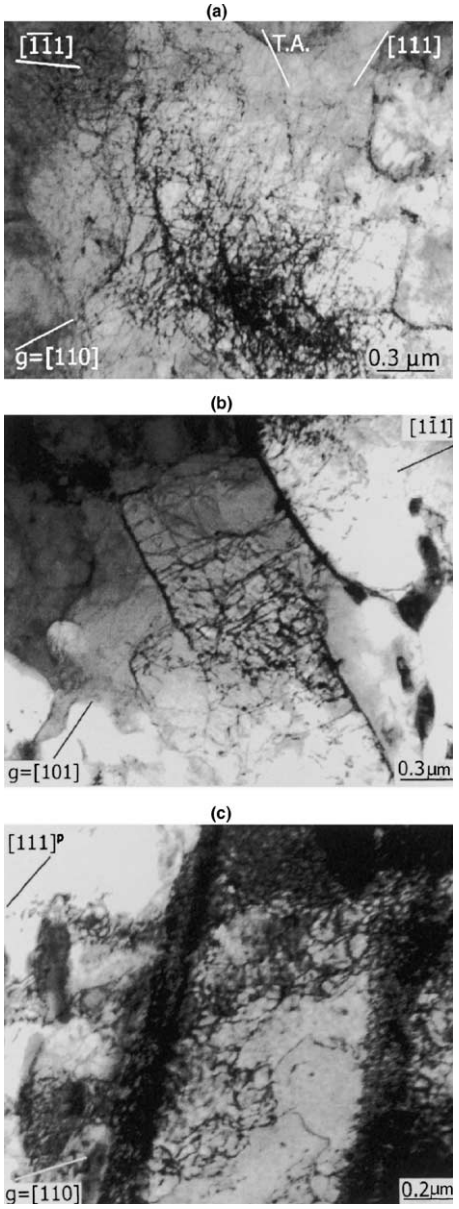

Fig. 6. Dislocation structure of a lath after 8% tensile test: (a) dislocation condensation into a wall, test temperature = −196 °C, beam direction [−5 5 4], g = [1 1 0]. t. a. is tensile axis and $[1\,1\,1]^{p}$ means the projection of the direction [1 1 1] into the image plane, the lath *c* axis is perpendicular to the foil plane; (b) interactions between dislocation wall and inter-lath carbides, test temperature = −196 °C, beam direction [−1 0 1], g = [1 0 1], the lath *c* axis is parallel to the foil plane; (c) two intra-lath tilt boundaries, test temperature = 0 °C, beam direction [−1 1 1], g = [1 1 0], the lath *c* axis is parallel to the foil plane.

is further noted that the number of small cracked inclusions is significantly increased as well.

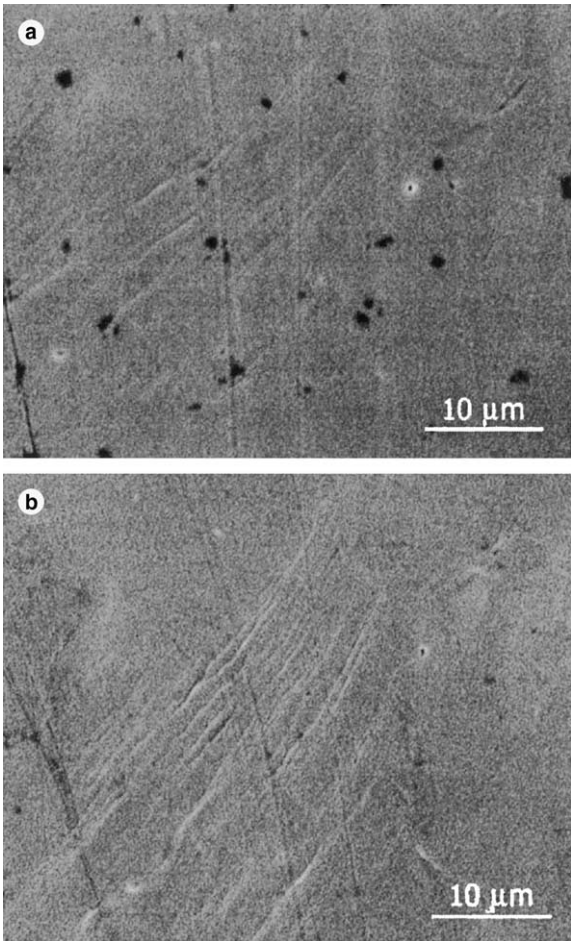

Fig. 7. Surface relief evolution in a specimen deformed to different amounts of plastic strain: (a) 2.5% and (b) 8%.

4. Discussion

The typical dislocation arrangements for liquid nitrogen temperature and plastic strain of 2.5% are made of uniformly distributed screw dislocations. In the observed laths oriented for single slip, screw dislocations with the four $a/2\langle 1\,1\,1\rangle$ Burgers vectors are present. This finding is in agreement with the well known intrinsic non-Schmidt effects in bcc metals (see for example [6,7]), which strongly contribute to multi-slip operation. It is also in agreement with the fact that dislocation microstructures become more homogeneous with decreasing grain size [8]. Namely, the complex stress state required by the strain compatibility between the thin laths would give rise to multiple slip.

At $T = -196$ °C, the strain hardening rate is relatively low, as compared to the room temperature behaviour of α-iron poly-crystals. At $T = 25$ °C, comparable data from the literature report strain hardening rates

two to five times larger [2]. From Fig. 2, the increase in flow stress between 2.5% and 8% strain is close to 100 MPa, which correspond to an averaged strain hardening rate $\Delta\sigma/\Delta\varepsilon$ of $(100\ \text{MPa}/5.5\times10^{-2})\approx 2$ GPa. The contribution of dislocation interactions (junction pinning) to the observed strain hardening rate can be estimated by differentiating

$$\sigma=\alpha\mu b\sqrt{\rho}\approx 10^{-10}\mu\sqrt{\rho}\quad\text{whence: }\frac{\Delta\sqrt{\rho}}{\Delta\varepsilon}\approx 2\times10^{10}\frac{1}{\mu}\frac{\Delta\sigma}{\Delta\varepsilon}.$$

Here, $\mu\approx 100$ GPa, which means $\Delta\rho\approx 5\times10^{14}\ \text{m}^{-2}$. The observations (see Fig. 6) are consistent with $\Delta\rho$ values rather comprised between 10^{13} and $10^{14}\ \text{m}^{-2}$. Therefore, dislocation interaction is not the only contribution to the observed increase in flow stress: a contribution from mobile dislocation locking is needed as well.

In addition, weak junction pinning is consistent with the presented TEM observations, as per the following arguments. If strong junctions were formed between dislocations from the primary (with b = $a/2[1\,1\,1]$) and secondary slip systems (with b = $a/2[-1\,1\,1]$) as in Fig. 4(a) and (b), about one pinning point or bow out would be present every 100 nm, in the primary slip plane. Since the dislocations in the primary slip system exhibit 500 nm long portions, i.e. without any pinning point, it can be concluded that the junctions formed between dislocations with the {1 1 1} type Burgers vector are relatively weak. Stronger junctions could possibly be formed between {1 1 1} and {1 1 2} type Burgers vector dislocations (according to line tension considerations), but the {1 1 2} type dislocations were not found after liquid nitrogen temperature testing. However, activation of {1 1 2} slip is possible at higher temperatures.

The sharp bow outs visible in Figs. 4(a), (c) and 5(a) nevertheless reveal the presence of strong pinning points. Since junction pinning is likely not the origin of these configurations (see the previous paragraph), they could instead be produced due to kink pair nucleation in different and conflicting slip planes (cross-kinks) [9]. Dislocation motion with cross-kink locking and subsequent unzipping is elsewhere known as debris drag [10]. The cross-kink unzipping process is accompanied by the emission of interstitial debris loops of various sizes. Such mechanism could be the origin of the numerous small dislocation loops as visible in Figs. 4(a), (c) and 5(a). The comparison between Fig. 5(a) and (b) clearly shows that an increased temperature results in both the reduction of the characteristic straight screw segment lengths and in enhanced debris emission (see Section 3). In other words, the number of cross-kinks per unit length of mobile dislocation scales with the test temperature. In certain conditions, this self-pinning mechanism can contributes to the exhaustion of the mobile dislocation density.[1] Additional exhaustion mechanisms thought to be present include locking at interfaces, foreign atoms and small inclusions.

When the plastic deformation is increased from 2.5% up to 8% at −196 °C, the dislocations have tendency to collect into clusters (compare Figs. 4 and 6). Other structures like tilt boundaries are very scarce at −196 °C, whereas they are very frequent at 0 °C (see Fig. 6(c)). Tilt boundary formation is an efficient stress relieving mechanism in tensile loading conditions therefore, the absence of tilt boundaries at low temperature is consistent with the presence of strong residual stresses within the laths. The same conclusion can be drawn from the shape of the dislocation bow-outs, particularly in Figs. 4(c) and 5(a). These dislocation cluster configurations are most probably related with very high tri-axial stress concentrations which can in turn initiate defects, like inclusion cracking for example (see Section 3.4).

Finally, the surface features revealed in SEM are in agreement with the dislocation structures and stress–strain behaviour as reported in this study. Namely, the markings keep the same wavy and localized character up to 8% plastic strain: no unexpected sign of dislocation activity is evidenced. Consequently, the hardening rate remains comparatively low, at low test temperatures.

5. Conclusions

From the study of dislocation structure and surface relief developed under uni-axial tension at temperature of −196 °C and 0 °C in bainitic pressure vessel steel 16MND5, the following conclusions can be drawn:

(1) Dislocation structure investigation and surface relief observation revealed important deformation heterogeneity in the material. Deformation is localized into specific zones made of different, contiguous lath packet arrangements. The volume fraction of regions exhibiting strain localization increases with increasing plastic strain.
(2) In the deformed laths (about 10% of the specimen volume fraction), the dislocations are distributed homogeneously at low applied plastic strain (2.5%) and gradually condense into sub-lath size clusters and walls, with increasing deformation (8%).
(3) The length of the straight screw portions is characteristic of the test temperature and the tested

[1] The strain hardening associated with such self-pinning mechanism is expected to increase with temperature.

material, for a fixed plastic strain. This length increases with the decreasing test temperature.

(4) The interactions between dislocations and inter-lath carbides are strong enough to block slip propagation across the lath boundaries.
(5) Higher intra-lath stress concentrations are expected at lower test temperatures, where tilt boundary formation is less frequent.
(6) Exhaustion of the mobile dislocation density is believed to be an important contribution to the observed strain hardening rate. However, the experiments presented here cannot establish the relative contributions of the different exhaustion mechanisms, such as locking at interfaces (and also at foreign atoms and small inclusions) and self-pinning due to cross-kink formation.

Acknowledgements

This work was financially supported by Contract Programme Recherche en Simulation des Matériaux pour les Réacteurs Nucléaires, a CEA-CNRS-EDF joint program and in part by the grant of the AS CR No. 1QS200410502. The TEM observations were performed in the CEA-SRMP laboratory. The authors wish to thank Dr L. Boulanger for his kind support.

References

[1] A.G. Pineau, The Mechanical Behavior of Materials (ICM9), Paper No. 71, 2003.
[2] A.S. Keh, S. Weissmann, Electron Microscopy and Strength of Crystals, Interscience, New York, 1963, p. 231.
[3] D.J. Dingley, D. McLean, Acta Metall. 15 (1967) 885.
[4] S. Renevey, S. Carassou, B. Marini, C. Eripret, A. Pineau, J. Phys. IV 6 (1996) C6-343.
[5] J. Gil Sevillano, P. Van Houte, E. Aernoudt, Progr. Mater. Sci. 25 (1980) 69.
[6] K. Ito, V. Vitek, Philos. Mag. A 81 (5) (2001) 1387.
[7] V. Vitek, M. Mrovec, J.L. Bassani, Mater. Sci. Eng. A 365 (1-2) (2004) 31.
[8] J.J. Gracio, J.V. Fernandes, J.H. Schmitt, Mater. Sci. Eng. A 118 (1989) 97.
[9] F. Louchet, B. Viguier, Philos. Mag. A 80 (2000) 765.
[10] J. Marian, W. Cai, V. Bulatov, Nature Mater. 3 (2004) 158.